

The Use of Nanofibers in Regenerative Endodontic Therapy—A Systematic Review

Sebastian Candrea^{1,2}, Alexandrina Muntean^{2,*}, Anida-Maria Băbțan¹, Antonia Boca^{1,3},
Claudia Nicoleta Feurdean¹, Ioana Roxana Bordea⁴, Adina Bianca Boșca⁵ and Aranka Ilea^{1,*}

- ¹ Department of Oral Rehabilitation, Faculty of Dentistry, “Iuliu Hațieganu” University of Medicine and Pharmacy, 400012 Cluj-Napoca, Romania; candreasebastian@yahoo.com (S.C.); anidamaria.babtan@gmail.com (A.-M.B.); toniboca07@gmail.com (A.B.); cbraitoru@yahoo.com (C.N.F.)
- ² Department of Paediatric Dentistry, “Iuliu Hațieganu” University of Medicine and Pharmacy, 400012 Cluj-Napoca, Romania
- ³ Department of Conservative Dentistry, Faculty of Dentistry, “Iuliu Hațieganu” University of Medicine and Pharmacy, 400012 Cluj-Napoca, Romania
- ⁴ Department of Oral Health, Faculty of Dentistry, “Iuliu Hațieganu” University of Medicine and Pharmacy, 400012 Cluj-Napoca, Romania; roxana.bordea@gmail.com
- ⁵ Department of Histology, Faculty of Medicine, “Iuliu Hațieganu” University of Medicine and Pharmacy, 400012 Cluj-Napoca, Romania; bianca.bosca@umfcluj.ro
- * Correspondence: alexandrina.muntean@umfcluj.ro (A.M.); aranka.ilea@umfcluj.ro (A.I.)

Abstract: Pulpal pathology in young permanent teeth, caused by dental caries or trauma, can lead to disruption of root formation, leaving the tooth with an uncertain prognosis. Current therapies for such cases present a number of limitations; thus, the aim of this article is to provide an overview on the use of nanofibers in endodontics. The search was conducted on two databases and eight articles met the inclusion criteria for this systematic review. Data on nanofiber production and fiber characteristics were extracted and systematized in tables. Moreover, the ability of novel scaffolds to deliver either drugs or different therapeutic agents without interfering with the products’ characteristics is analyzed from the in vitro and in vivo data. The potential for nanofiber-based scaffolds to induce cellular differentiation and overcome the limitations of classic regenerative endodontic treatment is also discussed.

Keywords: nanofibers; endodontic therapy; electrospinning; tissue engineering; 3D scaffolds



Citation: Candrea, S.; Muntean, A.; Băbțan, A.-M.; Boca, A.; Feurdean, C.N.; Bordea, I.R.; Boșca, A.B.; Ilea, A. The Use of Nanofibers in Regenerative Endodontic Therapy—A Systematic Review. *Fibers* **2024**, *12*, 42. <https://doi.org/10.3390/fib12050042>

Academic Editor: Martin J. D. Clift

Received: 31 August 2023

Revised: 16 January 2024

Accepted: 8 May 2024

Published: 13 May 2024



Copyright: © 2024 by the authors. Licensee MDPI, Basel, Switzerland. This article is an open access article distributed under the terms and conditions of the Creative Commons Attribution (CC BY) license (<https://creativecommons.org/licenses/by/4.0/>).

1. Introduction

Dental caries is a multifactorial infectious disease in which the oral microbiome’s shift into acidogenic and acid tolerant bacteria plays a decisive role. It can affect the tooth’s structure during the eruption phase, leading to pulpal pathology before the root has fully developed [1,2].

The bacterial biofilm on the dental surface contains salivary proteins and glycoproteins that compose the pellicle, the associated microorganisms and their products, components derived from gingival sulcus fluid and blood, and food debris [3].

The acquired pellicle enables the attachment of oral bacteria, thus promoting the formation of the dental biofilm, and also limits the acid diffusion, playing the role of a physical barrier. Furthermore, microorganisms can be maintained close to the surface by weak transient van der Waal forces, without covalent or ionic interactions between the bacterial wall and the components in the biofilm [3,4]. Bacterial attachment can be reinforced by permanent bonds between the adhesins expressed by the bacteria and the specialized receptors in the acquired biofilm [4,5].

During the acquired pellicle buildup, *Streptococcus* and *Actinomyces* species act as early colonizers due to the expression of surface receptors that enable the direct link to the dental biofilm glycoproteins. Subsequently, other species, such as the *Veillonella* genus,

provide a favorable substrate for further attachment of later colonizers, thus leading to a culmination in microorganisms colonization [4,6].

Due to particular features such as a low external mineral content, high pulp–mineralized tissue ratio, deep occlusal pits, and fissures, young permanent teeth are prone to develop rampant caries. These rapidly-progressing caries frequently overcome the dentin deposition and infect the pulpal tissue, affecting the root development [7,8]. Consequently, the high fracture risk and improper crown-to-root ratio have a negative impact on the life span of affected teeth [9].

The endodontic management of pulp necrosis in young permanent teeth is challenging. The classic approach conforms with the principles of apexification; this method consists of the application of a calcium hydroxide dressing in the root canal in order to promote apical closure and to enable subsequent filling with gutta-percha [10,11]. This method has some limitations due to the need for repeated calcium hydroxide applications that come with multiple dental office visits and higher costs. A more recent therapeutic option consists of producing a quick apical barrier through the application of a bio-ceramic-based material (e.g., mineral trioxide aggregate—MTA) as an apical plug, thus shortening the treatment time [11,12].

The limitations of the aforementioned therapies can be overcome using the evoked bleeding (EB) strategy, which promotes dentinal wall thickening, as well as root lengthening [13,14]. The aim of this therapy is to obtain a microbial-free environment (a good disinfection) within the endodontic system and to produce apical bleeding, which enables stem cells' recruitment and differentiation into odontoblasts [15,16]. The blood clot acts as a scaffold for the apical stem cells and the dentinal proteins induce their differentiation into odontoblasts [17,18].

The disinfection of the endodontic system is usually achieved through calcium hydroxide dressing and/or antibiotic paste dressing [19]. Calcium hydroxide is an excellent endodontic disinfectant when applied into the main root canal, but its effectiveness within the depth of thin dentinal tubules is poor, due to low solubility, on the one hand [20], and the buffer capacity, on the other hand [21].

Triple antibiotic paste (TAP) offers good disinfection, but it potentially inhibits the revascularization of the newly formed pulpal tissue. Improper vascularization could interfere with stem cells' differentiations and could also result in dentin discoloration [22–24]. TAP, which was based on metronidazole (MET), ciprofloxacin (CIP), and minocycline (MINO) has been replaced by a double-antibiotic paste (DAP); in order to avoid dentin discoloration, MINO was excluded [25,26]. Moreover, antibiotic pastes are difficult to remove from the endodontic system [27], and, due to the acid pH, TAP could promote dentin decalcification after prolonged use [28].

In the past, regenerative endodontics took advantage of tissue engineering principles for managing non-vital young permanent teeth. The key to success in tissue engineering therapies is the use of three elements: stem cells, bioactive molecules such as growth factors, and scaffolds [9,14].

The use of nanofiber-based scaffolds with simple compositions or loaded with antibiotics and/or cellular inducing factors has been suggested as an alternative to TAP due to better dosage of the delivered antibiotic [29,30].

The aim of this paper is to provide a comprehensive review on current data regarding the endodontic therapy of young permanent teeth diagnosed with pulpal necrosis, in relation to nanofiber technology.

2. Materials and Methods

The current article is based on the search of two databases: PubMed and Mesh.

The search was conducted using the following Boolean search terms:

1. #1—"Nanofibers"[Mesh] OR "Nanofibers"[tw] OR "Tissue Scaffolds"[Mesh];
2. #2—"Endodontics"[Mesh] OR "Regenerative Endodontics"[Mesh] OR "Root Canal Preparation"[Mesh];

3. #3—(“Nanofibers”[Mesh] OR “Nanofibers”[tw] OR “Tissue Scaffolds”[Mesh]) AND (“Endodontics”[Mesh] OR “Regenerative Endodontics”[Mesh] OR “Root Canal Preparation”[Mesh]).

The articles eligible for inclusion in this review were assessed by two independent researchers.

The including criteria required the studies to be conducted using nanofibers as a scaffold for either disinfection purposes or cellular inductivity, or both. The use of hard dental tissue, dental stem cells, or oral bacteria was mandatory either in vivo or in vitro. The time period searched was the last ten years and articles had to be written in English. Additionally, review articles were excluded.

The data assessment focused on the type of nanofibers used, their manufacturing process, antimicrobial activity, cellular-inductive potential, and the most relevant data offered by the paper.

3. Results

The used search terms provided a total of 76 articles that were further processed by the title and abstract. After the article’s selection, a number of eight scientific papers met the inclusion criteria and were included in this review.

The overall statistics are as follows: reports sought for retrieval (n = 56); reports not retrieved (n = 1); reports assessed for eligibility (n = 55); reports excluded: Did not present nanofiber containing scaffolds (n = 47); and studies included in review (n = 8).

The data collected are summarized in Tables 1–4.

Table 1. Data systematization showing the types of scaffolds used.

Nr. crt/Citation	Authors	Year of Publication	Study Design	Control Scaffold/s	Test Scaffold/s
1/[29]	Bottino et al.	2013	in vitro	polydioxanone (PDS)	polydioxanone (PDS) with antibiotics
2/[30]	Palasuk et al.	2014	in vitro	polydioxanone (PDS)	polydioxanone (PDS) with antibiotics
3/[31]	Bottino et al.	2015	in vitro	polydioxanone (PDS)	Scaffolds with halloysite aluminosilicate clay nanotubes (HNTs); groups being 0.5, 3, 5, 10 wt%
4/[32]	Kamocki et al.	2015	in vitro	Polydioxanone (PDS)—negative control; saturated CIP/MET solution (i.e., 50 mg of each antibiotic in 1 mL) (DAP)—positive control	polydioxanone (PDS) with antibiotics
5/[33]	Pankajakshan et al.	2016	in vitro	Untreated dentin specimens—negative control; polydioxanone (PDS)—control; triple antibiotic solution (TAP solution, 50 mg/mL)—positive control.	polydioxanone (PDS) with antibiotics
6/[24]	Bottino et al.	2019	in vitro and in vivo (canine model)	in vitro [polydioxanone (PDS)—negative control; triple antibiotic paste (TAP)—positive control]; in vivo [evoked bleeding method (EB)]	polydioxanone (PDS) with antibiotics

Table 1. Cont.

Nr. crt/Citation	Authors	Year of Publication	Study Design	Control Scaffold/s	Test Scaffold/s
7/[34]	Moonesi Rad et al.	2019	in vitro	cellulose acetate/oxidized pullulan/gelatin (CA/ox-PULL/GEL)	boron (B)-modified bioactive glass nanoparticles (BG-NPs) based on cellulose acetate/oxidized pullulan/gelatin (CA/ox-PULL/GEL); groups being: 7%, 14%, 21% substitution of SiO ₂ with B ₂ O ₃
8/[35]	Leite et al.	2022	in vitro	[tubular scaffold poly(caprolactone) (TB-SC)]—negative control; [tubular scaffold poly(caprolactone) associated with fibronectin (FN) (TB-SC + FN)]—positive control	tubular scaffold poly(caprolactone) associated with collagen hydrogel (TB-SC + H); tubular scaffold poly(caprolactone) associated with FN-coated collagen hydrogel (TB-SC + HFN)

Table 2. Data systematization showing scaffold obtaining parameters and characteristics.

Nr. crt/Citation	Fiber Production Method/Parameters	Fiber Morphology Assessment	Chemical Structure Assessment	Mechanical Properties Assessment	Fiber Porosity
1/[29]	electrospinning/—2 mL/h, 18-cm distance, 15 kV	Scanning electron microscopy (SEM)	Fourier-transform infrared spectroscopy (FTIR)	Tensile strength testing	NA
2/[30]	electrospinning/—2 mL/h, 18-cm distance, 15 kV	Scanning electron microscopy (SEM)	Fourier transform infrared spectroscopy (FTIR)	Uniaxial tensile testing	NA
3/[31]	electrospinning/—2 mL/h, 20-cm distance, 15 kV	Scanning electron microscopy (SEM)	Fourier-transform infrared spectroscopy (FTIR)	Uniaxial microtensile testing	Transmission electron microscopy (TEM)
4/[32]	electrospinning/—2 mL/h, 18 cm distance, 15–18 kV.	Scanning electron microscopy (SEM)	NA	NA	NA
5/[33]	electrospinning/—2 mL/h, 18-cm distance, 15–19 kV	NA	NA	NA	NA
6/[24]	electrospinning/—2 mL/h, 18-cm distance, 15–19 kV	Scanning electron microscopy (SEM)	Fourier-transform infrared spectroscopy (FTIR)	Tensile strength testing	NA
7/[34]	thermally induced phase separation and porogen leaching/aluminum plate and foam; one direction freezing and freeze-drying; KCl leaching	Scanning electron microscopy (SEM)	Alizarin Red staining-distribution of BG-NPs	Compression test at 25% of strain in the stress-strain curve	Mercury porosimetry device
8/[35]	electrospinning/—1 mL/h, 18-cm distance, 12–13 kV	NA	NA	NA	NA

Table 3. Data systematization showing antimicrobials and pathogens used.

Nr. crt/Citation	Fiber Degradation/Water Absorption Assessment	Drug Release Assessment	Antimicrobials/ Concentration	Microbials	Antimicrobial Potential Evaluation
1/[29]	NA	High-performance liquid chromatography (HPLC)	Metronidazole (MET)/5 and 25 wt%; Ciprofloxacin (CIP)/5 and 25 wt%	<i>Porphyromonas gingivalis</i> (Pg) <i>Enterococcus faecalis</i> (Ef)	biofilm; agar diffusion assays
2/[30]	NA	NA	Metronidazole (MET), Ciprofloxacin (CIP) and combination of the two (3:1 MET/CIP, 1:1 MET/CIP and 1:3 MET/CIP)—25 wt%	Ef, Pg, <i>Fusobacterium nucleatum</i> (Fn)	agar diffusion testing
3/[31]	NA	NA	NA	NA	NA
4/[32]	NA	High-performance liquid chromatography (HPLC)	Metronidazole (MET), Ciprofloxacin (CIP) and combination of the two (3:1 MET/CIP, 1:1 MET/CIP and 1:3 MET/CIP)—25 wt%	NA	NA
5/[33]	NA	NA	Metronidazole (MET), Minocycline (MINO), and Ciprofloxacin (CIP)—30 wt%	An, Pg	fluorescent LIVE/DEAD BacLight Bacterial Viability Kit L-7012; confocal laser scanning microscopy (CLSM)
6/[24]	NA	NA	Metronidazole (MET), Ciprofloxacin (CIP), and Minocycline (MINO)—35 mg/mL (35 wt.%)	<i>Actinomyces naeslundii</i> (An)	in vitro—[confocal laser scanning microscopy (CLSM) and SEM]
7/[34]	Phosphate-buffered solution (PBS) for one month	NA	NA	NA	NA
8/[35]	NA	NA	NA	NA	NA

Pg—*Porphyromonas gingivalis*, Ef—*Enterococcus faecalis*, An—*Actinomyces naeslundii*, Fn—*Fusobacterium nucleatum*.

Table 4. Data systematization showing cellular effect assessment and the main results.

Nr. crt/Citation	Cell Viability/Differentiation/ Proliferation/Cytotoxicity Assessment	Main Results
1/[29]	International Organization for Standardization—toxicity assessment	<ul style="list-style-type: none"> • MET at 25 wt% and CIP (at 5 and 25 wt%) significantly reduced the diameter of the fiber compared with control. • No difference in tensile strength between dry and wet samples/CIP had significantly lower strength modulus compared with other groups. • In the first 48 h, the amount of released drug was close to a quarter regarding CIP and half for MET. • No significant difference in the inhibitory effect of the 5 wt% CIP compared with 25 wt% CIP, but 25 wt% CIP showed adverse effects at cellular level.

Table 4. Cont.

Nr. crt/Citation	Cell Viability/Differentiation/ Proliferation/Cytotoxicity Assessment	Main Results
2/[30]	CellTiter 96 AQueous One Solution Reagent—cell viability	<ul style="list-style-type: none"> • Micro/nanofibrous network—all groups; • The diameter of the fiber in antibiotic-containing scaffolds considerably smaller than control; • 1:1 MET/CIP scaffold had significantly higher tensile strength compared with control; • All the other groups had tensile strengths similar to control; • Scaffolds containing the antibiotic showed inhibitory effect on Ef, Pg, and Fn growth; contrarily, the MET-only group had no inhibitory effect on Pg and Fn; • On day 1, the 1:1 MET/CIP group significantly decreased cell viability compared with control and with other test groups; • After two weeks, cell viability was significantly higher in MET-only group compared with CIP-only group.
3/[31]	Water-soluble tetrazolium-1 assay—assess mitochondrial dehydrogenase activities; SEM-cell-scaffold interaction	<ul style="list-style-type: none"> • 3D porous network of the scaffold; • Diameter of fibers for 10 wt% HNTs was significantly higher and had a broader distribution; • Dry PDS and scaffolds based on 0.5 wt% HNT/PDS showed significant increase in tensile strength; • Increasing the HNT loading determined significantly lower strength for the hydrated PDS–HNTs; • Control showed significantly higher modulus; • Scaffolds promoted cell adherence and proliferation.
4/[32]	WST-1 assay-proliferation; LIVE/DEAD assay/calcein and ethidium homodimer (EthD-1)-cell viability	<ul style="list-style-type: none"> • Mean fiber diameter in the antibiotic-containing scaffolds was smaller compared with pure PDS; • In all samples, the burst drug(s) release was observed during the first 24 h; • Linear concentration throughout 14 days; • MET was released quicker than CIP (all of MET released by day 5); CIP had a release range from 30% to 60% in 14 days; • In all groups exposed to CIP-containing scaffolds, cell proliferation was significantly inhibited, depending on the concentration; • MET and pure PDS did not induce significant changes in cell proliferation; cell proliferation and viability were not affected by MET-only containing scaffolds; • CIP-containing scaffolds induced higher % of dead cells.
5/[33]	SEM and confocal laser scanning microscopy (CLSM)-cell adhesion and cytoskeletal morphology; CellTiter 96 AQueous One Solution Cell Proliferation Assay-cell proliferation	<ul style="list-style-type: none"> • Tested scaffold efficiently eliminated viable bacteria. • Enhanced hDPSCs adhesion and spreading-on test and control but delayed on TAP. SEM investigation demonstrated cell-covered dentin after 7 days for the control and test, but cells on TAP-treated dentin showed irregular morphology after 7 days. • Cellular proliferation was significantly higher on dentin conditioned with triple antibiotic-containing nanofibers after 7 days than TAP.

Table 4. Cont.

Nr. crt/Citation	Cell Viability/Differentiation/ Proliferation/Cytotoxicity Assessment	Main Results
6/[24]	in vivo/ex vivo-[hematoxylin–eosin (H&E) staining and light microscopy]	<p>in vitro</p> <ul style="list-style-type: none"> • Triple antibiotic eluting fibers showed a more homogeneous fiber distribution; • Antibiotic-free nanofiber showed increased strength and medium flexibility, in all tested conditions; • Triple antibiotic-eluting constructs (TA-3DC) have resulted 99.1% to 99.94% dead bacteria; • TAP completely eliminated viable bacterial with no statistically significant difference between TAP and TA-3DC <p>in vivo</p> <ul style="list-style-type: none"> • Teeth treated with TAP had almost complete radicular apexification; • In teeth treated with TA-3DC, bacterial load was reduced; hard tissue continued to form and radicular apexification was complete.
7/[34]	Alamar Blue Assay/microplate spectrophotometer-cell viability; SEM analysis/Confocal laser scanning microscopy analysis-cell morphology on the scaffolds; ALP activity/intracellular calcium/Alizarin Red staining-calcium deposition; immunohistochemical and histological staining (DSPP, OPN and Col I-proteins)-odontogenic differentiation/formation of dentin-like hard tissue;	<ul style="list-style-type: none"> • At 30 days B7–10—the lowest weight loss, B0–20—the highest weight loss, control/moderate weight loss; • Addition of BG-NPs resulted in lower weight reduction in scaffolds in the first week; • First day after immersion into PBS, water absorption (WA)% had the highest value in all groups, with WA capacity decreasing in parallel with weight loss; • Even distribution of BG-NPs within scaffolds; • Scaffolds were completely covered with minerals; homogeneity and thickness were directly proportional to time; • Pore sizes—5 to 200 μm; • Average porosity percentage—91.6%; • Increasing BG-NPs content resulted in reduced porosity percentage; • Optimal mechanical properties due to BG-NPs incorporation; • Cell viability was higher due to increased BG-NPs content of scaffolds; • Cell viability was higher due to B incorporation; • No difference in ALP enzyme activity in different scaffolds; • After two weeks, control had lower enzymatic activity than test; • Cells in test showed more extended and flattened morphology on the scaffolds compared with control; • BG-NPs incorporated in the scaffolds promoted calcium deposition, particularly in B-BG-NP positive staining of DSPP, OPN, and Col I-proteins in all groups and expression was higher in groups containing B-BG-NPs.
8/[35]	Alamar Blue solution/fluorescence reading-cell viability; genes evaluation: ITGA5, ITGAV, COL1A1 and COL3A1 by quantitative polymerase chain reaction (qPCR); Cell migration-fluorescence microscopy	<ul style="list-style-type: none"> • Cell proliferation in TB-SC + HFN group was significantly higher in comparison with all other groups; • In both study groups and in positive control group, genes ITGA5, ITGAV, COL1A1, and COL3A1 were upregulated in comparison to negative control; • TB-SC + HFN significantly upregulated the expression of COL1A1 and COL3A1 markers in comparison with all other groups; • Cell migration was significantly higher in all groups, compared to negative control.

The PRISMA flow chart reveals the selection stage (Figure 1).

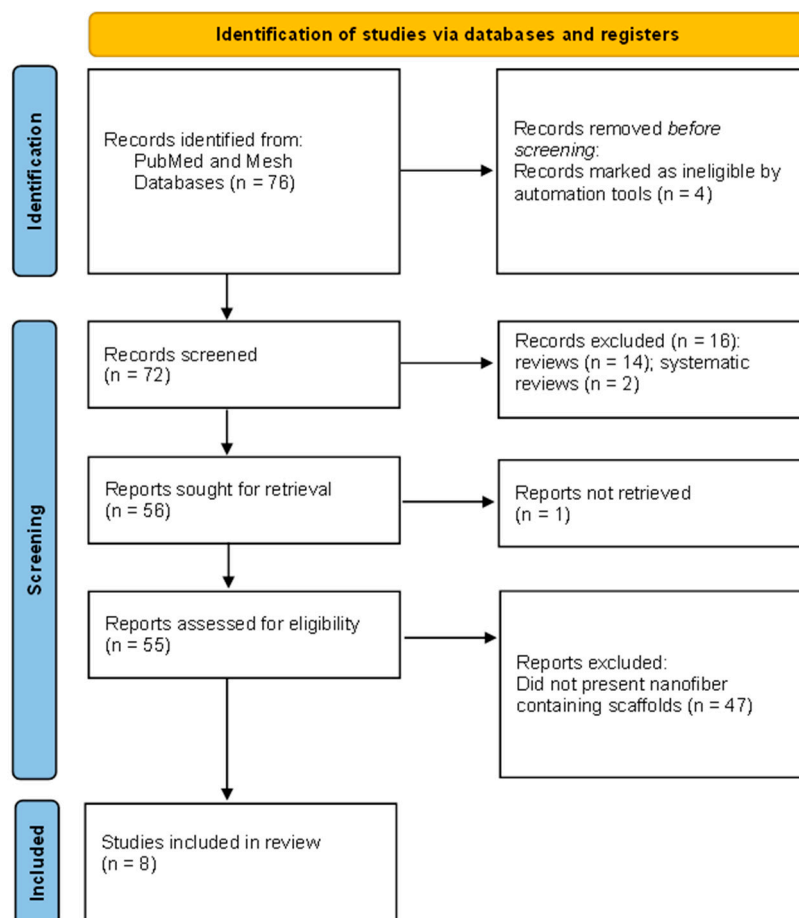


Figure 1. Identification of studies via databases.

4. Discussion

The included articles were published between 2013 and 2022 and were based on studies mainly conducted *in vitro*, with only one *in vivo* research-oriented article on a canine model [24]. The use of nanofiber-based scaffolds for endodontic purposes was mentioned earlier in the literature, e.g., the use of poly(epsilon-caprolactone) (PCL)/gelatin scaffolds mentioned by Yang et al. [36]. They reported promising results regarding hard tissue formation when the matrix loaded with human-derived pulp cells (hDPCs) was subcutaneously inserted in mice.

Polydioxanone is a polyester that resembles the PCL and polylactic acid (PLA) and presents excellent biodegradability as well as biocompatibility due to ester bonds. Moreover, the ester bonds provided great flexibility and relatively low mechanical strength [37]. This product disintegrated much faster than the other mentioned polymers and released less acidic products [38].

4.1. Nanofiber Obtaining Process, Characteristics, and Dynamics

Our data revealed that the most frequently used polymer was PDS by electrospinning and with the electrospun parameters set between 1 and 2 mL/h rate of injection 18–20 cm distance from the injection point to the collector device, and 12–19 KV power supply.

Electrospinning is a high-voltage-dependent method of producing nanofibers from a natural or synthetic polymer-based solution; these nanofibers closely resemble the tissue extracellular matrix [31,39]. This technique is based on inducing a strong potential difference between the polymer solution flowing through a narrow tip and a metallic collector.

By this method, an uneven arrangement of the fibers in the scaffold as well as scaffolds with aligned fibers were obtained [40].

Polydioxanone used in the studies was mainly derived from the suture material that contained PDS in a monofilament form [24,29,31]. The PDS was loaded with either antimicrobials, metronidazole (MET), ciprofloxacin (CIP), and minocycline (MINO) or with halloysite aluminosilicate clay nanotubes (HNTs) for scaffold production [31], and all combinations produced homogenous 3D scaffolds evaluated under scanning electron microscopy (SEM). The HNTs belong to the kaolinite family and contain aluminum and silica particles, used for drug or growth factor delivery. Cationic and anionic drugs can be loaded on HNT-containing scaffolds due to negatively charged silica present on the outer surface of the nanotubes and positively charged aluminum present in the lumen of the tubes [41,42].

The scaffold-containing triple antibiotics offer a more homogenous aspect than simple PDS [24]. An explanation could rely on the more hydrophilic nature of the antimicrobial-loaded solution, thus making it less viscous, altering the resultant electrospinning fibers [43,44]. If the solution presented a low viscosity, the jet turned into droplets; on the other hand, if the solution had a too high viscosity, it was difficult to pump through the capillary and dried on the tip [40].

The same idea could be applied to nanofibers loaded with HNTs, which offered significant increases in the fiber diameter and a broader distribution for 10 wt% HNTs but higher tensile strength for 0.5 wt% [31]. Once the amount of HNTs was higher, the viscosity of the solution changed, consequently reducing the scaffold's strength [42,44]. Besides viscosity, the conglomeration of HNTs in stress points along the nanofibers could be responsible for the loss of strength [45].

Bottino et al. [29] and Palasuk et al. [30] obtained a decrease in fiber diameter when two antibiotics, MET and CIP, were added to the scaffold. The fiber diameter is an important parameter of the scaffold, playing essential roles in the mechanical resistance as well as in the drug-release process. Addition of CIP to the fiber could result in a decrease in the material's strength and a reduction in drug release, explained by the difference in molecular weight (M_w) between antimicrobials, since CIP's M_w is almost double MET's M_w [46]. Moreover, according to the literature, a smaller diameter fiber offered a larger surface area for cellular adhesion and enabled a more gradual release of drugs loaded in the scaffold [47,48].

Moonesi Rad et al. [34] used the thermally induced phase separation method to obtain a three-dimensional scaffold. They obtained boron (B)-modified bioactive glass nanoparticles (BG-NPs) containing a cellulose acetate/oxidized pullulan/gelatin (CA/ox-PULL/GEL) scaffold. This method was based on the fact that the polymer containing solution was thermodynamically unstable. Thus, when the solution's temperature was lowered, it separated into a polymer-rich phase and a solvent-rich phase [49,50]. The solvent was then extracted using another solvent that could be sublimated, and the porogen material (KCl) was leached out; subsequently, the remaining nanofibers' porous structure was freeze-dried [34,51].

The above-mentioned authors reported obtaining a scaffold with an even distribution of BG-NPs and with lower weight loss when compared with BG-NP free scaffolds at the solubility assessment. This aspect could have derived from the release of alkali ions from the bio-glass particles that were capable of neutralizing the acidic product derived from the dissolution of the polymeric scaffold, as the authors explained; therefore, a decrease in solubility could be obtained by increasing the bio-glass in the scaffold [34]. Additionally, the water absorbance (WA) of the scaffold was enhanced by the bio-glass addition due to the hydrophilic properties of the material and the weak bonds between the fiber and the glass [52,53].

It is worth mentioning the deposition of hard minerals on the scaffold when submersed into simulated body fluid (SBF). The deposition of calcium and phosphate was uniformly distributed. The explanation resides in the bio-glass negative charge and the silica ions,

offering a nucleation point for the mineral deposition. The replacement of silica oxide with boron oxide enhanced the deposition of apatite crystals due to the opening of the scaffold's structure [54,55].

The addition of BG-NPs enhanced the mechanical properties of the scaffold but decreased its porosity. The balance between the mechanical resistance and the porosity of the scaffold had to be maintained, since larger pores promoted the development of mineralized tissue in the bio-material, but it impaired the strength of the scaffold, making it difficult to manipulate [56].

4.2. Antimicrobial Assessment

Five of the eight articles included in this review investigated the antimicrobial loading on the nanofiber scaffold and four studies assessed the antimicrobial activity of the scaffolds. The antibacterial substances (i.e., MET, CIP, and MINO) were integrated in the scaffold in the range of 5 wt% to 35 wt%. An initial drug release burst was observed in the first 24 to 48 h, with MET presenting a steeper release: up to 50% during the first two days [29]. The antibiotic-containing fibers became hydrophilic, being easier to degrade progressively through hydrolysis, and thus sustaining the therapeutic drug release [24,57]. Another important parameter to be taken in consideration is the pH. MET's dissolution could influence CIP release from the fibers. MET's solubility was indirectly proportional to the pH, with a minimum solubility at pH = 8, whereas CIP had optimal solubility at neutral pH. Thus, the dosage ratio of the two drugs should be taken in consideration [58,59].

Notably, the electrospinning method used for obtaining the scaffold did not affect the properties of the antimicrobials [29]. This aspect was in accordance with the literature regarding other antimicrobials (example: diclofenac sodium or indomethacin) or growth factors [60–62].

The microbial species investigated were the main endodontic pathogens found in cases of dental pulp gangrene and are often responsible for failure of endodontic treatment (e.g., Ef) [8,63,64].

According to the data, MET-only scaffolds failed to be effective against the pathogens, whereas TAP-containing scaffolds (35 wt%) presented efficiency comparable to TAP paste against *Actinomyces naeslundii* (An) and the mix of MET and CIP also showed efficiency against the studied pathogens [24,29,30,33].

4.3. Cell Viability, Differentiation, Proliferation, and Toxicity Assessment

All studies evaluated the performance of nanofiber scaffolds in relation to stem cells (hDPSCs) for in vitro studies, or cells harvested through the EB method for in vivo studies [24,29,31,39].

Antibiotic-containing scaffolds demonstrated good biocompatibility, similar to simple scaffolds, without associated antimicrobials. When antibiotics were administered into the root canal using nanofiber-based scaffolds, drug release was better controlled and in lower concentrations (5 wt% MET = 386 µg, 25 wt% MET = 1.38 mg, 5 wt% CIP = 280 µg, and 25 wt% CIP = 1 mg) [29], compared to administration as TAP paste (1 g/mL). The literature cites toxic cellular effects of antibiotic concentrations exceeding 1 g/mL; the survival rate of cells derived from the apical papillae increased only below this concentration [26,65].

Remarkably, MET presented less cytotoxicity than CIP. Even though MET has been shown to have cytotoxic effects directly related to the concentration used [66,67], it seemed to enhance the viability of hDPSCs, as observed by Kamoki et al. [32]. The explanation could be that MET promoted cell proliferation through a cytokine-mediated inflammatory response [68]. Fluoroquinolones, group of antimicrobials that include CIP, are notorious cytotoxic substances [69]; thus, the negative impact of CIT on cell proliferation and viability is easily comprehended. On the other hand, Bottino et al. [29] evidenced that CIP-containing PDS scaffolds had equally effective antibacterial properties in concentrations of both 25 wt% and 5 wt%; thus, loading the nanofibers with a reduced quantity of CIP, but at an effective dosage, could be the answer for cell viability.

Similar to TAP, the *in vivo* use of PDS scaffolds loaded with antimicrobials promoted apical closure through an osseous dentin-like tissue, although an inflammatory infiltrate was reported in the apical area [24]. The dental pulp stem cells had a lesser potential of differentiation into odontoblasts than cells derived from the apical papillae, which were more likely to survive the disinfection protocol [70]. Growth factors and differentiation determining growth factors are known to be found in the dentinal tissue [28,71] and antimicrobial therapy had a negative impact on the release of these factors; thus, formation of osteoblast like cells was more likely to occur [18,24].

The use of HNTs in the scaffold revealed enhanced cellular proliferation of the hDP-SCs. HNT scaffolds proved good biocompatibility toward other cellular lines, such as osteoblasts and fibroblasts [72]. Halloysite nanotubes presented the capacity to encapsulate antimicrobials, being able to prevent the initial drug burst release from the fibers [73].

Even with no disinfection potential, PCL-based nanofiber-containing scaffolds associated with fibronectin (FN)-coated collagen hydrogel had higher cellular proliferation, chemotaxis, and gene expression of pulp regeneration markers than PCL nanofibers [35]. The biocompatibility, wound healing, and enhanced protein secretion of collagen and fibronectin was evidenced in the literature toward dental pulp cells, as well as other cell types (e.g., hepatocytes) [74–76].

Another promoter of cellular differentiation proved to be the scaffold loaded with bio-glass nanoparticles and boron [34]. Alkaline phosphatase (ALP)'s increased activity demonstrated that hDPSCs differentiated into odontoblasts [77]. Moreover, confocal laser scanning microscopy analysis (CSLM) revealed the presence of cellular processes in the newly differentiated cells, a characteristic of odontoblasts [78].

Also, the differentiation markers investigated by Moonesi Rad et al. [34] through immune-histochemical methods revealed greater expression in the bio-glass boron-enriched-containing scaffolds. Collagen type I, which represents the main protein in the dentinal matrix [79], as well as dentin phosphoprotein (DPP)—the main non-collagenous protein—and osteopontin (OPN) [80], proved the odontoblastic differentiation [81].

4.4. Challenges and Future Research

Future research should focus on developing three-dimensional scaffolds based on materials with high biocompatibility, which enables stem cell cultivation or recruitment, also promoting cell growth and controlling cell differentiation. Such three-dimensional matrices should facilitate the influx of nutrients deep into the scaffold, as well as efflux of metabolites. Additionally, the synthetic matrices should be biodegradable with no toxic effect on human cells, so that the newly formed tissue could produce its own matrix.

Advanced endodontic therapies should focus on fully restoring the dental pulp, with all the morphological and functional characteristics. One possibility for achieving this ideal is to develop a scaffold that already contains various types of pre-differentiated stem cells in its structure. Maybe the way to truly regenerate the pulpal–dentin complex throughout the endodontic system is to create a microenvironment suitable for cell survival and not necessarily for cell differentiation, since the latter is more environmentally sensitive.

In line with the aforementioned ideas, cell insemination should be achieved by adding the cells in layers to obtain constructs with a characteristic architecture that mimics the natural tissue (e.g., blood and lymphatic vascular circulation, nerve fibers, etc.). The idea of loading the scaffolds with antimicrobials in non-toxic doses should also be considered, since the sterilization of the endodontic root canal system is difficult to obtain. Another aspect to be taken in consideration is the possibility of performing the endodontic therapy in such a manner that the tooth structure is not weakened, which could increase the risk of dental fracture, leading to therapeutic failure.

In summary, the articles cited in this review reveal that the clinical scenario of dental pulp necrosis can be mimicked by introducing biofilm-derived bacteria into the root canals and demonstrated that the use of nanofiber scaffolds loaded with antibiotics in a much lower concentration could be as effective as the use of TAP [24]. Bottino et al.

also reported that the use of antibiotic-loaded scaffolds proved as efficient as DAP [30]. Nanofiber scaffolds composed of PDS as a carrier also ensured a drug-efficient dosage against common endodontic pathogens [29,33]. All studies demonstrated the antibacterial efficiency of scaffolds against the biofilm, in balance with the capability of modulating cell differentiation. Through the support provided to the non-differentiated cells, scaffolds could act as an inducer of cell differentiation. Moreover, the inductive properties of scaffolds could be improved by the addition of cell growth factors such as fibronectin and collagen [35]. Leite et al. used a PCL scaffold associated with fibronectin and collagen hydrogel to stimulate the migration and proliferation of hDPSCs, and cell differentiation was highlighted through expression of pulp regeneration markers [35]. Promising results regarding modulation of stem cells' function was obtained by the addition of B and BGNPs to a cellulose-based scaffold obtained through phase separation. The authors reported superior biological properties of the scaffold for controlling cell differentiation, demonstrated by the expression of marker proteins and the deposition of hard tissue on the scaffold [34]. The ability of delivering bioactive agents to the endodontic system could be optimized through the addition of HNTs to a PDS scaffold. The hollow tube can be used as a carrier for a wide variety of substances for cell modulation and bacterial control [31].

5. Conclusions

Several *in vitro* and *in vivo* studies reported promising results regarding the use of scaffolds for endodontic treatment. The nanofiber-based scaffolds offer a tremendous advantage through possible loading with different materials and drugs compared with the classic TAP revitalization method. The fiber properties, antimicrobial potential, and cellular impact of the scaffold reveal the start of a new era in endodontic therapy in young permanent teeth. In conclusion, nanofiber-based scaffolds could represent an alternative to current endodontic therapies, but further *in vivo* studies should be conducted for a better understanding of the scaffolds' advantages and limitations.

Author Contributions: Conceptualization: S.C., A.M. and A.I.; methodology, I.R.B., A.B.B. and A.I.; investigation, S.C., A.-M.B. and A.B.; writing—original draft preparation, S.C., A.-M.B. and C.N.F.; project administration, A.M.; writing—review and editing, A.M., A.B.B. and A.I.; data curation, A.B. and A.B.B.; resources, C.N.F., I.R.B. and A.B.B.; supervision, I.R.B. and A.I. All authors have read and agreed to the published version of the manuscript.

Funding: This research was funded by Ministry of Research, Innovation and Digitization, CNCS—UEFISCDI, project number PN-III-P4-PCE-2021-1140, within PNCDI III, a financial support for which the authors are thankful.

Conflicts of Interest: The authors declare no conflict of interest.

Abbreviations

Abbreviation	Meaning
MTA	Mineral trioxide aggregate
EB	Evoked bleeding
TAP	Triple antibiotic paste
MET	Metronidazole
CIP	Ciprofloxacin
MINO	Minocycline
DAP	Double antibiotic paste
PDS	Polydioxanone
HNTs	Halloysite aluminosilicate clay nanotubes
TB-SC	Tubular scaffold poly(caprolactone)
FN	Fibronectin
H	Collagen hydrogel
CA/ox-PULL/GEL	Cellulose acetate/oxidized pullulan/gelatin
BGNPs	Bioactive glass nanoparticles

Abbreviation	Meaning
B-BGNPs	Boron-modified bioactive glass nanoparticles
B	Boron
SEM	Scanning electron microscopy
FTIR	Fourier-transform infrared spectroscopy
TEM	Transmission electron microscopy
HPLC	High-performance liquid chromatography
Pg	<i>Porphyromonas gingivalis</i>
Ef	<i>Enterococcus faecalis</i>
An	<i>Actinomyces naeslundii</i>
Fn	<i>Fusobacterium nucleatum</i>
CLSM	Confocal laser scanning microscopy
PBS	Phosphate-buffered solution
H&E	Hematoxylin–eosin
TA-3DC	Triple antibiotic-eluting constructs
qPCR	Quantitative polymerase chain reaction
EthD-1	Ethidium homodimer
WA	Water absorption
ALP	Alkaline phosphatase
DPP	Dentin phosphoprotein
DSPP	Dentin sialophosphoprotein
OPN	Osteopontin
ITGA5, ITGAV	Genes that encode the protein integrin α 5 and α V
COL1A1, COL3A1	Genes that encode collagen type I and III
hDPSCs	Human-derived pulp cells
PCL	Poly(epsilon caprolactone)
PLA	Poly(lactic acid)
PGA	Poly(glycolic acid)
Mw	Molecular weight
SBF	Simulated body fluid

References

- Tanner, A.C.R.; Kressirer, C.A.; Faller, L.L. Understanding Caries from the Oral Microbiome Perspective. *J. Calif. Dent. Assoc.* **2016**, *44*, 437–446. [\[CrossRef\]](#)
- Tong, H.J.; Seremidi, K.; Stratigaki, E.; Kloukos, D.; Duggal, M.; Gizani, S. Deep Dentine Caries Management of Immature Permanent Posterior Teeth with Vital Pulp: A Systematic Review and Meta-Analysis. *J. Dent.* **2022**, *124*, 104214. [\[CrossRef\]](#)
- Chawhuaveang, D.D.; Yu, O.Y.; Yin, I.X.; Lam, W.Y.-H.; Mei, M.L.; Chu, C.-H. Acquired Salivary Pellicle and Oral Diseases: A Literature Review. *J. Dent. Sci.* **2021**, *16*, 523–529. [\[CrossRef\]](#)
- Huang, R.; Li, M.; Gregory, R.L. Bacterial Interactions in Dental Biofilm. *Virulence* **2011**, *2*, 435–444. [\[CrossRef\]](#)
- Arweiler, N.B.; Netuschil, L. The Oral Microbiota. In *Microbiota of the Human Body*; Schwierz, A., Ed.; Advances in Experimental Medicine and Biology; Springer International Publishing: Cham, Switzerland, 2016; Volume 902, pp. 45–60, ISBN 978-3-319-31246-0.
- Nobbs, A.H.; Lamont, R.J.; Jenkinson, H.F. Streptococcus Adherence and Colonization. *Microbiol. Mol. Biol. Rev. MMBR* **2009**, *73*, 407–450. [\[CrossRef\]](#)
- Carvalho, J.C. Caries Process on Occlusal Surfaces: Evolving Evidence and Understanding. *Caries Res.* **2014**, *48*, 339–346. [\[CrossRef\]](#)
- Nagata, J.Y.; Soares, A.J.; Souza-Filho, F.J.; Zaia, A.A.; Ferraz, C.C.R.; Almeida, J.F.A.; Gomes, B.P.F.A. Microbial Evaluation of Traumatized Teeth Treated with Triple Antibiotic Paste or Calcium Hydroxide with 2% Chlorhexidine Gel in Pulp Revascularization. *J. Endod.* **2014**, *40*, 778–783. [\[CrossRef\]](#)
- Albuquerque, M.T.P.; Valera, M.C.; Nakashima, M.; Nör, J.E.; Bottino, M.C. Tissue-Engineering-Based Strategies for Regenerative Endodontics. *J. Dent. Res.* **2014**, *93*, 1222–1231. [\[CrossRef\]](#)
- Bottino, M.C.; Pankajakshan, D.; Nör, J.E. Advanced Scaffolds for Dental Pulp and Periodontal Regeneration. *Dent. Clin. N. Am.* **2017**, *61*, 689–711. [\[CrossRef\]](#)
- Trope, M. Treatment of the Immature Tooth with a Non-Vital Pulp and Apical Periodontitis. *Dent. Clin. N. Am.* **2010**, *54*, 313–324. [\[CrossRef\]](#)

12. Diogenes, A.; Ruparel, N.B. Regenerative Endodontic Procedures: Clinical Outcomes. *Dent. Clin. N. Am.* **2017**, *61*, 111–125. [[CrossRef](#)]
13. Galler, K.M. Clinical Procedures for Revitalization: Current Knowledge and Considerations. *Int. Endod. J.* **2016**, *49*, 926–936. [[CrossRef](#)]
14. Diogenes, A.; Henry, M.A.; Teixeira, F.B.; Hargreaves, K.M. An Update on Clinical Regenerative Endodontics. *Endod. Top.* **2013**, *28*, 2–23. [[CrossRef](#)]
15. Namour, M.; Theys, S. Pulp Revascularization of Immature Permanent Teeth: A Review of the Literature and a Proposal of a New Clinical Protocol. *Sci. World J.* **2014**, *2014*, 737503. [[CrossRef](#)]
16. Torabinejad, M.; Nosrat, A.; Verma, P.; Udochukwu, O. Regenerative Endodontic Treatment or Mineral Trioxide Aggregate Apical Plug in Teeth with Necrotic Pulps and Open Apices: A Systematic Review and Meta-Analysis. *J. Endod.* **2017**, *43*, 1806–1820. [[CrossRef](#)]
17. Ostby, B.N. The Role of the Blood Clot in Endodontic Therapy. An Experimental Histologic Study. *Acta Odontol. Scand.* **1961**, *19*, 324–353. [[CrossRef](#)]
18. Galler, K.M.; Buchalla, W.; Hiller, K.-A.; Federlin, M.; Eidt, A.; Schiefersteiner, M.; Schmalz, G. Influence of Root Canal Disinfectants on Growth Factor Release from Dentin. *J. Endod.* **2015**, *41*, 363–368. [[CrossRef](#)]
19. Ribeiro, J.S.; Münchow, E.A.; Ferreira Bordini, E.A.; de Oliveira da Rosa, W.L.; Bottino, M.C. Antimicrobial Therapeutics in Regenerative Endodontics: A Scoping Review. *J. Endod.* **2020**, *46*, S115–S127. [[CrossRef](#)]
20. Ercan, E.; Dalli, M.; Dülgergil, C.T. In Vitro Assessment of the Effectiveness of Chlorhexidine Gel and Calcium Hydroxide Paste with Chlorhexidine against *Enterococcus Faecalis* and *Candida Albicans*. *Oral Surg. Oral Med. Oral Pathol. Oral Radiol. Endod.* **2006**, *102*, e27–e31. [[CrossRef](#)]
21. Portenier, I.; Haapasalo, H.; Rye, A.; Waltimo, T.; Ørstavik, D.; Haapasalo, M. Inactivation of Root Canal Medicaments by Dentine, Hydroxylapatite and Bovine Serum Albumin. *Int. Endod. J.* **2001**, *34*, 184–188. [[CrossRef](#)]
22. Dubey, N.; Xu, J.; Zhang, Z.; Nör, J.E.; Bottino, M.C. Comparative Evaluation of the Cytotoxic and Angiogenic Effects of Minocycline and Clindamycin: An In Vitro Study. *J. Endod.* **2019**, *45*, 882–889. [[CrossRef](#)]
23. Porter, M.L.A.; Münchow, E.A.; Albuquerque, M.T.P.; Spolnik, K.J.; Hara, A.T.; Bottino, M.C. Effects of Novel 3-Dimensional Antibiotic-Containing Electrospun Scaffolds on Dentin Discoloration. *J. Endod.* **2016**, *42*, 106–112. [[CrossRef](#)]
24. Bottino, M.C.; Albuquerque, M.T.P.; Azabi, A.; Münchow, E.A.; Spolnik, K.J.; Nör, J.E.; Edwards, P.C. A Novel Patient-Specific Three-Dimensional Drug Delivery Construct for Regenerative Endodontics. *J. Biomed. Mater. Res. B Appl. Biomater.* **2019**, *107*, 1576–1586. [[CrossRef](#)]
25. Reynolds, K.; Johnson, J.D.; Cohenca, N. Pulp Revascularization of Necrotic Bilateral Bicuspid Using a Modified Novel Technique to Eliminate Potential Coronal Discolouration: A Case Report. *Int. Endod. J.* **2009**, *42*, 84–92. [[CrossRef](#)]
26. Ruparel, N.B.; Teixeira, F.B.; Ferraz, C.C.R.; Diogenes, A. Direct Effect of Intracanal Medicaments on Survival of Stem Cells of the Apical Papilla. *J. Endod.* **2012**, *38*, 1372–1375. [[CrossRef](#)]
27. Berkhoff, J.A.; Chen, P.B.; Teixeira, F.B.; Diogenes, A. Evaluation of Triple Antibiotic Paste Removal by Different Irrigation Procedures. *J. Endod.* **2014**, *40*, 1172–1177. [[CrossRef](#)]
28. Yassen, G.H.; Eckert, G.J.; Platt, J.A. Effect of Intracanal Medicaments Used in Endodontic Regeneration Procedures on Microhardness and Chemical Structure of Dentin. *Restor. Dent. Endod.* **2015**, *40*, 104–112. [[CrossRef](#)]
29. Bottino, M.C.; Kamocki, K.; Yassen, G.H.; Platt, J.A.; Vail, M.M.; Ehrlich, Y.; Spolnik, K.J.; Gregory, R.L. Bioactive Nanofibrous Scaffolds for Regenerative Endodontics. *J. Dent. Res.* **2013**, *92*, 963–969. [[CrossRef](#)]
30. Palasuk, J.; Kamocki, K.; Hippenmeyer, L.; Platt, J.A.; Spolnik, K.J.; Gregory, R.L.; Bottino, M.C. Bimix Antimicrobial Scaffolds for Regenerative Endodontics. *J. Endod.* **2014**, *40*, 1879–1884. [[CrossRef](#)]
31. Bottino, M.C.; Yassen, G.H.; Platt, J.A.; Labban, N.; Windsor, L.J.; Spolnik, K.J.; Bressiani, A.H.A. A Novel Three-Dimensional Scaffold for Regenerative Endodontics: Materials and Biological Characterizations. *J. Tissue Eng. Regen. Med.* **2015**, *9*, E116–E123. [[CrossRef](#)]
32. Kamocki, K.; Nör, J.E.; Bottino, M.C. Dental Pulp Stem Cell Responses to Novel Antibiotic-Containing Scaffolds for Regenerative Endodontics. *Int. Endod. J.* **2015**, *48*, 1147–1156. [[CrossRef](#)]
33. Pankajakshan, D.; Albuquerque, M.T.P.; Evans, J.D.; Kamocka, M.M.; Gregory, R.L.; Bottino, M.C. Triple Antibiotic Polymer Nanofibers for Intracanal Drug Delivery: Effects on Dual Species Biofilm and Cell Function. *J. Endod.* **2016**, *42*, 1490–1495. [[CrossRef](#)]
34. Moonesi Rad, R.; Atila, D.; Akgün, E.E.; Evis, Z.; Keskin, D.; Tezcaner, A. Evaluation of Human Dental Pulp Stem Cells Behavior on a Novel Nanobiocomposite Scaffold Prepared for Regenerative Endodontics. *Mater. Sci. Eng. C Mater. Biol. Appl.* **2019**, *100*, 928–948. [[CrossRef](#)]
35. Leite, M.L.; de Oliveira Ribeiro, R.A.; Soares, D.G.; Hebling, J.; de Souza Costa, C.A. Poly(Caprolactone)-Aligned Nanofibers Associated with Fibronectin-Loaded Collagen Hydrogel as a Potent Bioactive Scaffold for Cell-Free Regenerative Endodontics. *Int. Endod. J.* **2022**, *55*, 1359–1371. [[CrossRef](#)]
36. Yang, X.; Yang, F.; Walboomers, X.F.; Bian, Z.; Fan, M.; Jansen, J.A. The Performance of Dental Pulp Stem Cells on Nanofibrous PCL/Gelatin/nHA Scaffolds. *J. Biomed. Mater. Res. A* **2010**, *93*, 247–257. [[CrossRef](#)]
37. Liu, X.; Feng, S.; Wang, X.; Qi, J.; Lei, D.; Li, Y.; Bai, W. Tuning the Mechanical Properties and Degradation Properties of Polydioxanone Isothermal Annealing. *Turk. J. Chem.* **2020**, *44*, 1430–1444. [[CrossRef](#)]

38. Panchal, S.S.; Vasava, D.V. Biodegradable Polymeric Materials: Synthetic Approach. *ACS Omega* **2020**, *5*, 4370–4379. [[CrossRef](#)]
39. Bottino, M.C.; Thomas, V.; Janowski, G.M. A Novel Spatially Designed and Functionally Graded Electrospun Membrane for Periodontal Regeneration. *Acta Biomater.* **2011**, *7*, 216–224. [[CrossRef](#)]
40. Zafar, M.; Najeeb, S.; Khurshid, Z.; Vazirzadeh, M.; Zohaib, S.; Najeeb, B.; Sefat, F. Potential of Electrospun Nanofibers for Biomedical and Dental Applications. *Materials* **2016**, *9*, 73. [[CrossRef](#)]
41. Lvov, Y.M.; Shchukin, D.G.; Möhwald, H.; Price, R.R. Halloysite Clay Nanotubes for Controlled Release of Protective Agents. *ACS Nano* **2008**, *2*, 814–820. [[CrossRef](#)]
42. Qi, R.; Cao, X.; Shen, M.; Guo, R.; Yu, J.; Shi, X. Biocompatibility of Electrospun Halloysite Nanotube-Doped Poly(Lactic-Co-Glycolic Acid) Composite Nanofibers. *J. Biomater. Sci. Polym. Ed.* **2012**, *23*, 299–313. [[CrossRef](#)]
43. Dargaville, B.L.; Vaquette, C.; Rasoul, F.; Cooper-White, J.J.; Campbell, J.H.; Whittaker, A.K. Electrospinning and Crosslinking of Low-Molecular-Weight Poly(Trimethylene Carbonate-Co-(L)-Lactide) as an Elastomeric Scaffold for Vascular Engineering. *Acta Biomater.* **2013**, *9*, 6885–6897. [[CrossRef](#)] [[PubMed](#)]
44. Haroosh, H.J.; Chaudhary, D.; Dong, Y. Electrospun PLA/PCL Fibers with Tubular Nanoclay: Morphological and Structural Analysis. *J. Appl. Polym. Sci.* **2012**, *124*, 3930–3939. [[CrossRef](#)]
45. Yang, F.; Both, S.K.; Yang, X.; Walboomers, X.F.; Jansen, J.A. Development of an Electrospun Nano-Apatite/PCL Composite Membrane for GTR/GBR Application. *Acta Biomater.* **2009**, *5*, 3295–3304. [[CrossRef](#)]
46. Tungprapa, S.; Jangchud, I.; Supaphol, P. Release Characteristics of Four Model Drugs from Drug-Loaded Electrospun Cellulose Acetate Fiber Mats. *Polymer* **2007**, *48*, 5030–5041. [[CrossRef](#)]
47. Kenawy, E.-R.; Abdel-Hay, F.I.; El-Newehy, M.H.; Wnek, G.E. Controlled Release of Ketoprofen from Electrospun Poly(Vinyl Alcohol) Nanofibers. *Mater. Sci. Eng. A* **2007**, *1–2*, 390–396. [[CrossRef](#)]
48. Kenawy, E.-R.; Abdel-Hay, F.I.; El-Newehy, M.H.; Wnek, G.E. Processing of Polymer Nanofibers through Electrospinning as Drug Delivery Systems. *Mater. Chem. Phys.* **2009**, *113*, 296–302. [[CrossRef](#)]
49. Gupte, M.J.; Ma, P.X. Nanofibrous Scaffolds for Dental and Craniofacial Applications. *J. Dent. Res.* **2012**, *91*, 227–234. [[CrossRef](#)]
50. Ma, P.X. Biomimetic Materials for Tissue Engineering. *Adv. Drug Deliv. Rev.* **2008**, *60*, 184–198. [[CrossRef](#)]
51. Wei, G.; Ma, P.X. Macroporous and Nanofibrous Polymer Scaffolds and Polymer/Bone-like Apatite Composite Scaffolds Generated by Sugar Spheres. *J. Biomed. Mater. Res. A* **2006**, *78*, 306–315. [[CrossRef](#)]
52. Lei, B.; Shin, K.-H.; Noh, D.-Y.; Jo, I.-H.; Koh, Y.-H.; Kim, H.-E.; Kim, S.E. Sol-Gel Derived Nanoscale Bioactive Glass (NBG) Particles Reinforced Poly(ϵ -Caprolactone) Composites for Bone Tissue Engineering. *Mater. Sci. Eng. C Mater. Biol. Appl.* **2013**, *33*, 1102–1108. [[CrossRef](#)]
53. Pourhaghgouy, M.; Zamanian, A. Ice-Templated Scaffolds of Bioglass Nanoparticles Reinforced-Chitosan. In Proceedings of the 2014 21th Iranian Conference on Biomedical Engineering (ICBME), Tehran, Iran, 26–28 November 2014; pp. 48–52. [[CrossRef](#)]
54. Tainio, J.; Paakinaho, K.; Ahola, N.; Hannula, M.; Hyttinen, J.; Kellomäki, M.; Massera, J. In Vitro Degradation of Borosilicate Bioactive Glass and Poly(L-Lactide-Co- ϵ -Caprolactone) Composite Scaffolds. *Materials* **2017**, *10*, 1274. [[CrossRef](#)] [[PubMed](#)]
55. Araujo, H.C.; Nakamune, A.C.M.S.; Garcia, W.G.; Pessan, J.P.; Antoniali, C. Carious Lesion Severity Induces Higher Antioxidant System Activity and Consequently Reduces Oxidative Damage in Children’s Saliva. *Oxid. Med. Cell. Longev.* **2020**, *2020*, 3695683. [[CrossRef](#)]
56. Mour, M.; Das, D.; Winkler, T.; Hoenig, E.; Mielke, G.; Morlock, M.M.; Schilling, A.F. Advances in Porous Biomaterials for Dental and Orthopaedic Applications. *Materials* **2010**, *3*, 2947–2974. [[CrossRef](#)]
57. Ferracane, J.L. Hygroscopic and Hydrolytic Effects in Dental Polymer Networks. *Dent. Mater.* **2006**, *22*, 211–222. [[CrossRef](#)]
58. Breda, S.A.; Jimenez-Kairuz, A.F.; Manzo, R.H.; Olivera, M.E. Solubility Behavior and Biopharmaceutical Classification of Novel High-Solubility Ciprofloxacin and Norfloxacin Pharmaceutical Derivatives. *Int. J. Pharm.* **2009**, *371*, 106–113. [[CrossRef](#)]
59. Rediguieri, C.F.; Porta, V.; Nunes, D.S.G.; Nunes, T.M.; Junginger, H.E.; Kopp, S.; Midha, K.K.; Shah, V.P.; Stavchansky, S.; Dressman, J.B.; et al. Biowaiver Monographs for Immediate Release Solid Oral Dosage Forms: Metronidazole. *J. Pharm. Sci.* **2011**, *100*, 1618–1627. [[CrossRef](#)]
60. Taepaiboon, P.; Ruktanonchai, U.; Supaphol, P. Drug-Loaded Electrospun Mats of Poly(Vinyl Alcohol) Fibres and Their Release Characteristics of Four Model Drugs. *Nanotechnology* **2006**, *17*, 2317–2329. [[CrossRef](#)]
61. Sahoo, S.; Ang, L.T.; Goh, J.C.-H.; Toh, S.-L. Growth Factor Delivery through Electrospun Nanofibers in Scaffolds for Tissue Engineering Applications. *J. Biomed. Mater. Res. A* **2010**, *93*, 1539–1550. [[CrossRef](#)]
62. Waeiss, R.A.; Negrini, T.C.; Arthur, R.A.; Bottino, M.C. Antimicrobial Effects of Drug-Containing Electrospun Matrices on Osteomyelitis-Associated Pathogens. *J. Oral Maxillofac. Surg.* **2014**, *72*, 1310–1319. [[CrossRef](#)]
63. Madhubala, M.M.; Srinivasan, N.; Ahamed, S. Comparative Evaluation of Propolis and Triantibiotic Mixture as an Intracanal Medicament against *Enterococcus Faecalis*. *J. Endod.* **2011**, *37*, 1287–1289. [[CrossRef](#)]
64. Pallotta, R.C.; Ribeiro, M.S.; de Lima Machado, M.E. Determination of the Minimum Inhibitory Concentration of Four Medicaments Used as Intracanal Medication. *Aust. Endod. J.* **2007**, *33*, 107–111. [[CrossRef](#)]
65. Chuensombat, S.; Khemaleelakul, S.; Chattipakorn, S.; Srisuwan, T. Cytotoxic Effects and Antibacterial Efficacy of a 3-Antibiotic Combination: An In Vitro Study. *J. Endod.* **2013**, *39*, 813–819. [[CrossRef](#)]
66. Chatzkel, J.A.; Vossough, A. Metronidazole-Induced Cerebellar Toxicity. *Pediatr. Radiol.* **2010**, *40*, 1453. [[CrossRef](#)]
67. Kuriyama, A.; Jackson, J.L.; Doi, A.; Kamiya, T. Metronidazole-Induced Central Nervous System Toxicity: A Systematic Review. *Clin. Neuropharmacol.* **2011**, *34*, 241–247. [[CrossRef](#)]

68. Rizzo, A.; Paolillo, R.; Guida, L.; Annunziata, M.; Bevilacqua, N.; Tufano, M.A. Effect of Metronidazole and Modulation of Cytokine Production on Human Periodontal Ligament Cells. *Int. Immunopharmacol.* **2010**, *10*, 744–750. [[CrossRef](#)]
69. Sobolewska, B.; Hofmann, J.; Spitzer, M.S.; Bartz-Schmidt, K.U.; Szurman, P.; Yoeruek, E. Antiproliferative and Cytotoxic Properties of Moxifloxacin on Rat Retinal Ganglion Cells. *Curr. Eye Res.* **2013**, *38*, 662–669. [[CrossRef](#)] [[PubMed](#)]
70. Tziafas, D.; Kodonas, K. Differentiation Potential of Dental Papilla, Dental Pulp, and Apical Papilla Progenitor Cells. *J. Endod.* **2010**, *36*, 781–789. [[CrossRef](#)]
71. Cassidy, N.; Fahey, M.; Prime, S.S.; Smith, A.J. Comparative Analysis of Transforming Growth Factor-Beta Isoforms 1-3 in Human and Rabbit Dentine Matrices. *Arch. Oral Biol.* **1997**, *42*, 219–223. [[CrossRef](#)]
72. Zhou, W.Y.; Guo, B.; Liu, M.; Liao, R.; Rabie, A.B.M.; Jia, D. Poly(Vinyl Alcohol)/Haloysite Nanotubes Bionanocomposite Films: Properties and in Vitro Osteoblasts and Fibroblasts Response. *J. Biomed. Mater. Res. A* **2010**, *93*, 1574–1587. [[CrossRef](#)]
73. Qi, R.; Shen, M.; Cao, X.; Zhang, L.; Xu, J.; Yu, J.; Shi, X. Electrospun Poly(Lactic-Co-Glycolic Acid)/Haloysite Nanotube Composite Nanofibers for Drug Encapsulation and Sustained Release. *J. Mater. Chem.* **2010**, *20*, 10622–10629. [[CrossRef](#)]
74. Kaufman, G.; Whitescarver, R.A.; Nunes, L.; Palmer, X.-L.; Skrtic, D.; Tutak, W. Effects of Protein-Coated Nanofibers on Conformation of Gingival Fibroblast Spheroids: Potential Utility for Connective Tissue Regeneration. *Biomed. Mater.* **2018**, *13*, 025006. [[CrossRef](#)]
75. Das, P.; DiVito, M.D.; Wertheim, J.A.; Tan, L.P. Collagen-I and Fibronectin Modified Three-Dimensional Electrospun PLGA Scaffolds for Long-Term In Vitro Maintenance of Functional Hepatocytes. *Mater. Sci. Eng. C Mater. Biol. Appl.* **2020**, *111*, 110723. [[CrossRef](#)] [[PubMed](#)]
76. Leite, M.L.; Soares, D.G.; Anovazzi, G.; Anselmi, C.; Hebling, J.; de Souza Costa, C.A. Fibronectin-Loaded Collagen/Gelatin Hydrogel Is a Potent Signaling Biomaterial for Dental Pulp Regeneration. *J. Endod.* **2021**, *47*, 1110–1117. [[CrossRef](#)]
77. Lee, J.-H.; Kang, M.-S.; Mahapatra, C.; Kim, H.-W. Effect of Aminated Mesoporous Bioactive Glass Nanoparticles on the Differentiation of Dental Pulp Stem Cells. *PLoS ONE* **2016**, *11*, e0150727. [[CrossRef](#)] [[PubMed](#)]
78. Cavalcanti, B.N.; Zeitlin, B.D.; Nör, J.E. A Hydrogel Scaffold That Maintains Viability and Supports Differentiation of Dental Pulp Stem Cells. *Dent. Mater.* **2013**, *29*, 97–102. [[CrossRef](#)] [[PubMed](#)]
79. Abrahão, I.J.; Martins, M.D.; Katayama, E.; Antoniazzi, J.H.; Segmentilli, A.; Marques, M.M. Collagen Analysis in Human Tooth Germ Papillae. *Braz. Dent. J.* **2006**, *17*, 208–212. [[CrossRef](#)]
80. Saito, K.; Nakatomi, M.; Ida-Yonemochi, H.; Ohshima, H. Osteopontin Is Essential for Type I Collagen Secretion in Reparative Dentin. *J. Dent. Res.* **2016**, *95*, 1034–1041. [[CrossRef](#)]
81. Deshpande, A.S.; Fang, P.-A.; Zhang, X.; Jayaraman, T.; Sfeir, C.; Beniash, E. Primary Structure and Phosphorylation of Dentin Matrix Protein 1 (DMP1) and Dentin Phosphophoryn (DPP) Uniquely Determine Their Role in Biomineralization. *Biomacromolecules* **2011**, *12*, 2933–2945. [[CrossRef](#)]

Disclaimer/Publisher’s Note: The statements, opinions and data contained in all publications are solely those of the individual author(s) and contributor(s) and not of MDPI and/or the editor(s). MDPI and/or the editor(s) disclaim responsibility for any injury to people or property resulting from any ideas, methods, instructions or products referred to in the content.